Application of Arbitrary Position and Width Pulse Trains Signals in Ultrasonic Imaging: Correlation Performance Study

L. Svilainis[1], K. Lukoseviciute[1], V. Dumbrava[1], A. Chaziachmetovas[1], A. Aleksandrovas[1]
[1]*Department of Signal Processing, Kaunas University of Technology,*
Studentu St. 50, LT-51368 Kaunas, Lithuania
linas.svilainis@ktu.lt

***Abstract*—Ultrasonic imaging requires both the accuracy and the resolution. Conventional imaging systems use the pulse signals to accomplish the task. But the energy attainable with such signals is limited. Spread spectrum, compressible signals allow to achieve the wide bandwidth even using long durations. Conventional signals do not offer full flexibility or, like nonlinear frequency modulation signals, lack the ease of properties control. We suggest using novel spread spectrum signals generation technique: trains of pulses of arbitrary pulse width and position (APWP). It is expected that APWP should have properties similar to chirp (wide, controllable bandwidth) and both the single pulse (low correlation sidelobes) signals. Study presented here was aimed at evaluating the correlation properties of APWP signals. It indicates that application of APWP signals allows obtaining the properties better or close to those of the conventional signals. It can be concluded that APWP signals offer a new perspective in imaging applications.**

***Index Terms*—High resolution imaging, ultrasonic measurement, ultrasonic imaging; spread spectrum, pulse compression methods.**

I. INTRODUCTION

Ultrasonic applications gained popularity thanks to small equipment size, environmental safety and cost-effectiveness. Ultrasonic imaging in medicine [1], [2] and non-destructive testing and evaluation [3]–[5] is the only technique offering the direct interaction with test media. While propagation time estimation accuracy depend on the signal energy, input noise and signal spectrum [6]–[8], imaging resolution depends on the envelope bandwidth [9]–[11]. In order to obtain both the accuracy and the resolution, high energy and wide bandwidth signals are needed. Conventional imaging systems use the high voltage pulse signals to accomplish the task. But the energy attainable with such signals is limited by the excitation voltage, which in turn is defined by transducer construction or excitation electronics. Spread spectrum (SS), compressible signals [12]–[14] allow to achieve the wide bandwidth even using long durations. After compression in matched filter (correlation processing) signal duration in reduced and the energy is concentrate at one time instant [15], [16]. Wideband signals can turn useful if applied for structural noise dispersion increase in composites imaging [17]. Another advantage offered by SS signals is the simultaneous probing ability thanks to availability of the orthogonal signals [16], [20]. Usually, linear frequency modulation (chirp) or arbitrary waveform signals are considered [4], [9] best candidates for SS. But chirp has rectangular spectrum which causes its correlation function to have large sidelobes [9]. Arbitrary waveform signals are not easy to generate if large voltages are needed [13]. Nonlinear frequency modulation (NFM) signals are gaining popularity thanks to the ability to control the shape of the spectrum [14] and the sidelobe level [15], [16]. But there is no convenient procedure for frequency modulation function rectification from desired properties. Therefore, NFM studies are being carried out by manually assigning various functions and looking for desired performance. Pulse signal exhibits best correlation sidelobes properties but do not possess the high energy and orthogonality properties of SS. We suggest using novel spread spectrum signals generation technique [18]: trains of arbitrary pulse width and position (APWP) pulses. It is expected that APWP should have properties similar to chirp (wide, controllable bandwidth) and both the single pulse (low correlation sidelobes) signals. Study presented below was aimed at evaluating the correlation properties of APWP signals.

II. APWP SIGNALS

The novel spectrum spread technique did not receive the proper attention in ultrasound: trains of the arbitrary position and width pulses (APWP) [18], [19]. Technique is using a chaotically placed train of square pulses with arbitrary position and width (Fig. 1).

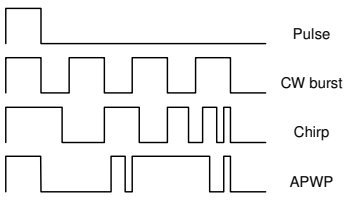

Fig. 1. Comparison on conventional and APWP signals.

The APWP signal can be treated as a mixture of the pulse

Manuscript received July 23, 2012; accepted October 27, 2012.
This research was funded by a grant (No. MIP-058/2012) from the Research Council of Lithuania.

width modulation (PWM) and the pulse position modulation (PPM). It is produced from the set of random duration pulses, where both pause and duration is guarded to be within the allowed range to construct the frequency components within desired range.

III. EXPERIMENT SETUP

Usual experimental setup would be expected to be carried out in real conditions. But in such case the variation of ultrasonic transducer of propagation media properties due to temperature would affect the transmission AC response. In addition, changing the excitation signal, upload to pulser memory and collection of new signals would take time. Therefore it was suggested to split the experiment into two parts: one was used for whole system AC response measurement, another was carried out numerically, using the former measurement results. Solid stainless steel block was placed into water tank and reflections of ultrasonic signals from the block were collected (Fig. 2). Wideband (86%) composite (48 dB sensitivity) ultrasonic transducer TF5C6N (supplied by Doppler Ltd.) with center frequency 4,61 MHz was used in pulse-echo mode.

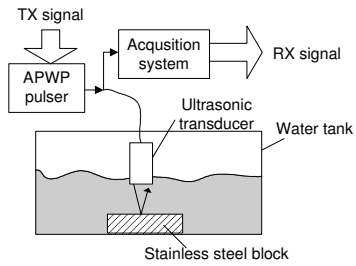

Fig. 2. System AC response measurement setup.

The received echo signal s_R can be treated as carrying the information about the whole system (pulser, ultrasonic transducer and acquisition system) transmission properties

$$S_R(\omega) = S_T(\omega) \cdot T_P(\omega) \cdot T_X(\omega) \cdot T_{ACQ}(\omega) + n(\omega), \quad (1)$$

where $T_P(t)$ is the transmission AC response of the pulser, $T_X(t)$ is the combined transmission AC response of the transducer in transmission, water path, reflection from interface and transducer in reception, $T_{ACQ}(t)$ is the transmission AC response of the whole acquisition system, including cables, preamplifier, filters and ADC response and $n(t)$ is a non-correlated additive white Gaussian noise (AWGN). Then, using the excitation signal $S_T(\omega)$ (obtained as Fourier transform of the mathematical representation of signal loaded into pulser memory) and the received echo signal $S_R(\omega)$ (obtained as the Fourier transform of the signal recorded in acquisition system memory) transmission AC response T_{sys} of the whole system can be obtained

$$T_{sys}(\omega) = \frac{S_R(\omega)}{S_T(\omega)}, \quad (2)$$

In order to reduce the noise influence and eliminate the spectral zeroes present in square signal spectrum, several records of different duration signals were averaged. Several excitation signals s_T were used in first part of the experiment: pulse signals of duration 10 ns to 200 ns (refer Fig. 3). Since chirp signals do not have spectral dips, such signals were also used for probing. Two types of chirp signals were used: 0.1 MHz to 20 MHz and 1 MHz to 15 MHz. System transmission AC response obtained using the chirp signals are presented in Fig. 4.

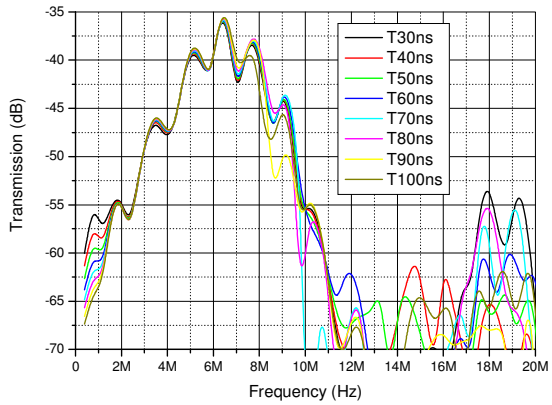

Fig. 3. System AC response when measured with square pulse.

All the obtained system transmission AC responses were combined to produce a single AC response (solid line in Fig. 4)

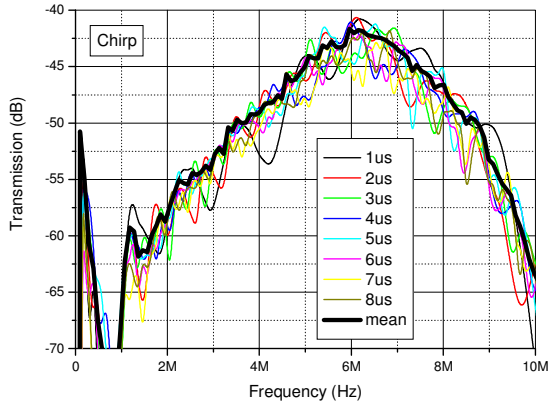

Fig. 4. System AC response when measured with chirp and mean value of all measurement (solid line).

This AC response T_{sys} was later used to obtain the received echo signal $S_R(\omega)$ for any candidate signal which was described mathematically

$$S_{Rnew}(\omega) = S_{Tnew}(\omega) \cdot T_{sys}(\omega). \quad (3)$$

Signal in frequency domain $S_R(\omega)$ was converted into time domain signal $s_R(t)$ using the inverse Fourier transform.

AC response analysis was used to establish the -6dB passband frequencies. From Fig. 4 data it was established that lowest passband frequency is 4.5 MHz and highest passband frequency is 8.1 MHz.

Three signals were used in succeeding experiments: square pulse, chirp and APWP (Fig. 1). The APWP signal was described as a sequence of the interleaving high and low level pulses of duration τ_n

$$s_T(t) = 1(\tau_1) + 0(\tau_2) + 1(\tau_3) + 0(\tau_4) + \ldots + 1(\tau_n) + 0(\tau_n), \quad (4)$$

Generation of durations τ_n was done using Monte Carlo

technique, using random generator with even distribution. Chirp signal was not optimized: it was assigned to span from 4.5 MHz to 8.1 MHz. Pulse signal was optimized by linearly varying the pulse duration and noting the best value of the convergence criteria. After optimisation procedure (1000000 Monte Carlo runs) signals (refer Fig. 5 for example signals after sidelobe energy optimisation) were submitted for further analysis.

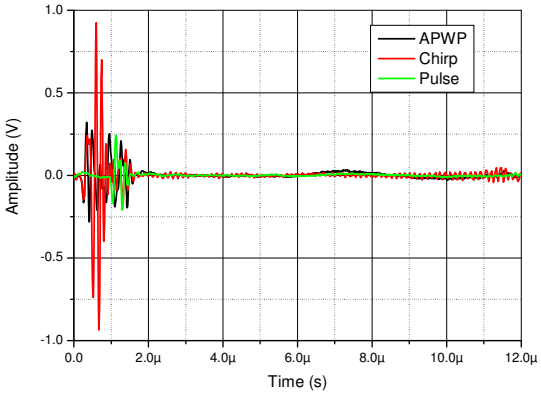

Fig. 5. Received signals after sidelobe energy optimisation.

Three convergence criteria, reflecting different correlation function properties were used: i) maximum value of the sidelobe (max(SL)); ii) sidelobe energy (E(SL)); iii) mainlobe duration τ_i (Fig. 6).

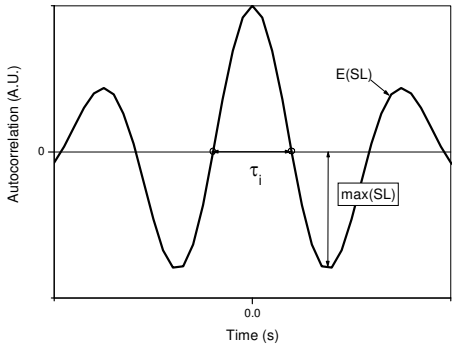

Fig. 6. Convergence criteria explanation: i) maximum value of the sidelobe (max(SL)); ii) sidelobe energy (E(SL)); iii) mainlobe duration τ_i.

These criteria were applied on autocorrelation function

$$R_m = \sum_{k=1}^{K} s_{k-m} \cdot s_k \ . \tag{5}$$

Maximum value was obtained by searching the maximum value to the left of the mainlobe (index 1 to m_L) and to the right (index m_R to M)

$$\max(SL) = \max\left(R_m\right)\Big|_{m=1\ldots mL \forall mR\ldots M} , \tag{6}$$

where m_L and m_R are leftmost and rightmost positions index of the mainlobe and M is autocorrelation function length.

Sidelobe energy was obtained by taking the L2 norm over the left side of the mainlobe (index 1 to m_L) and to the right (index m_R to M).

$$E(SL) = \sum_m \left(R_m\right)^2\Big|_{m=1\ldots mL \forall mR\ldots M} . \tag{7}$$

Mainlobe duration was obtained as the difference between index m_L and m_R with subsample interpolation using linear approximation.

IV. Experiment Results

Three Monte Carlo runs with different convergence criteria were run. Results for sidelobe peaks level (max(SL)) optimisation are presented in Table 1 and Fig. 7 and Fig. 8.

TABLE I. Results for sidelobe maximum optimisation.

Signal type	max(SL),a.u.	E(SL),a.u.	τ_I, ns
APWP	0.22	2.06	118.1
Chirp	0.80	3.67	79.2
Pulse	0.33	1.30	113.6

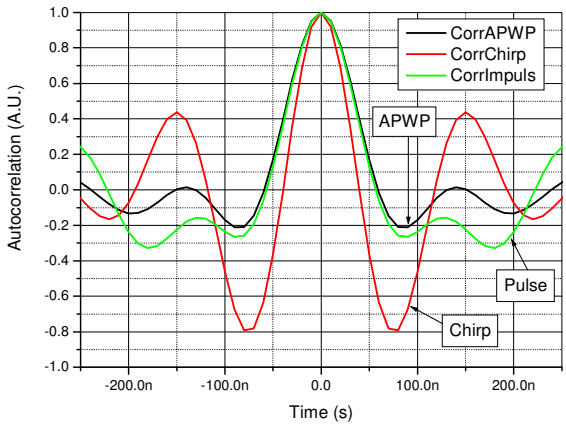

Fig. 7. Autocorrelation function in mainlobe proximity (zoom-in) after sidelobes' maximum level optimisation.

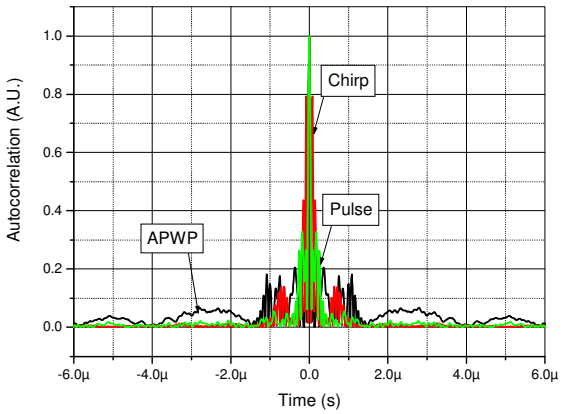

Fig. 8. Autocorrelation function envelope in mainlobe proximity (zoom-out) after sidelobes' maximum level optimisation.

It can be seen, that APWP signal outperforms the last two, has much better correlation properties.

Results for sidelobe energy (E(SL)) optimisation are presented in Table II and Fig. 9.

TABLE II. Results for sidelobe energy optimisation.

Signal type	max(SL),a.u.	E(SL),a.u.	τ_I, ns
APWP	0.37	1.34	108.3
Chirp	0.80	3.66	79.2
Pulse	0.33	1.30	113.6

It can be seen (Fig. 9), that though square pulse signal outperforms the last two, APWP signal has much better correlation properties than chirp signal. Again, chirp signal has shortest mainlobe width.

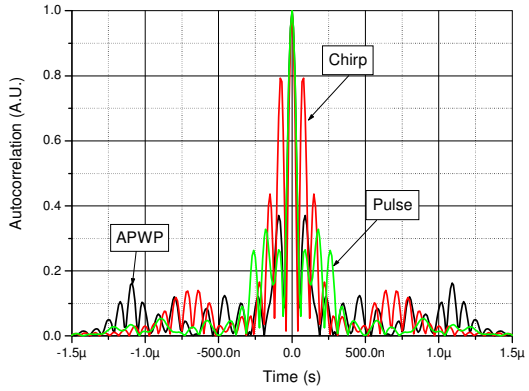

Fig. 9. Autocorrelation function envelope Hilbert (zoom-out) after sidelobes' energy minimisation.

Results for mainlobe width (duration τ_i) optimisation are presented in Table III and Fig. 10.

TABLE III. RESULTS FOR MAINLOBE DURATION OPTIMISATION.

Signal type	max(SL),a.u.	E(SL),a.u.	τ_I, ns
APWP	0.79431	9.09402	75.7
Chirp	0.80345	3.66467	79.2
Pulse	0.77544	3.29871	80.0

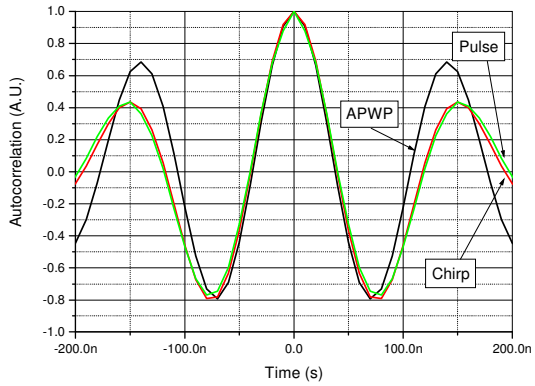

Fig. 10. Autocorrelation function in mainlobe proximity (zoom-in) after mainlobes' width minimisation.

Here, all signals have similar performance. Though, APWP signal has slightly better correlation properties than the other two.

V. CONCLUSIONS

A preliminary study indicates that application of APWP signals allows obtaining the properties better or close to those of the conventional signals. In case sidelobe of peaks level optimisation APWP signal outperforms the last two, has much better correlation properties. In case of the sidelobe energy optimisation, though square pulse signal outperforms the rest of the signals, APWP signal has much better correlation properties than chirp signal. In case of the mainlobe width optimisation all signals have similar performance. Though, APWP signal has slightly better correlation properties than the other two. It can be concluded that APWP signals offer a new perspective in imaging applications.

REFERENCES

[1] P. N. T. Wells, "Ultrasonic imaging of the human body", *Rep. Prog. Phys.*, vol. 62, no. 5, pp. 671–722. 1999. [Online]. Available: http://dx.doi.org/10.1088/0034-4885/62/5/201

[2] R. A. Harris, D. H. Follett, M. Halliwell, et al., "Ultimate limits in ultrasonic imaging resolution" *Ultrasound in Medicine & Biology*, vol. 17, no. 6, pp. 547–558, 1991. [Online]. Available: http://dx.doi.org/10.1016/0301-5629(91)90025-R

[3] Y. Zhou, G. Petculescu, I. Komsky, S. Krishnaswamy, "A high-resolution real-time ultrasonic imaging system for NDI applications", *Health Monitoring and Smart Nondestructive Evaluation of Structural and Biological Systems SPIE,* vol. 6177, pp. 17717–17717, 2006.

[4] S. J. Wen, X. D. Chen, J. Bao, D. Y. Yu, "Ultrasonic transmitter for coded excitation in medical endoscope imaging system", in *Proc. of the Int. symp. Photoelectronic detection and imaging SPIE*, 2008, vol. 6622, pp. 62217–62217.

[5] T. Hutt, F. Simonetti, "Experimental observation of super-resolution imaging in highly attenuative materials", *Medical imaging SPIE*, vol. 7968, 2011.

[6] Q. F. Li, X. H. Jin, M. Zhao, L. H. Shi, Z. X. Shao, "Simulation on Improving Imaging Resolution of SAFT", in *Proc. of the International Conference on Measuring Technology And Mechatronics Automation*, 2009, vol. II, pp. 351–354. [Online]. Available: http://dx.doi.org/10.1109/ICMTMA.2009.590

[7] X. D. Chen, H. Zhou, S. J. Wen, D. Y, Yu, "Increasing average power in medical ultrasonic endoscope imaging system by coded excitation", in *Proc. of the Int. Conf. On Optical Instruments and Technology: Optical Systems and Optoelectronic Instruments SPIE*, 2009, vol. 7156.

[8] L. R. Varshney, D. Thomas, "Sidelobe Reduction for Matched Filter Range Processing", in *Proc. IEEE Radar Conf.*, 2003, pp. 446–451.

[9] Y. K. Chan, M. Y. Chua, and V. C. Koo, "Sidelobes Reduction Using Simple Two And Tri-Stages Non Linear Frequency Modulation (NLFM)", *Progress In Electromagnetics Research*, vol. 98, pp. 33–52, 2009. [Online]. Available: http://dx.doi.org/10.2528/PIER09073004

[10] E. Behradfar, A. Mahloojifar, A. E. Behradfar, "Performance Enhancement of Coded Excitation in Ultrasonic B-mode Images" in *Proc. of the IEEE Second Int. Conf. on Machine Vision*, pp. 220–224, 2009.

[11] D. E. Rani, K. SriDevi, "Mainlobe Width Reduction Using Linear and Nonlinear Frequency Modulation", in *Proc. of the Int. Conf. on Advances in Recent Technologies in Communication and Computing*, 2009, pp. 918–920.

[12] L. Meng-Lin, G. Wei-Jung, L. Pai-Chi, "Sidelobe reduction for synthetic aperture focusing in high-frequency ultrasonic imaging", in *Proc.of the IEEE Symposium on Ultrasonics*, 2003, vol. 2, pp. 1557–1560.

[13] J. Cowe, E. Boni, S. Ricci, P. Tortoli, D. H. Evans, "Coded excitation can provide simultaneous improvements in sensitivity and axial resolution in Doppler ultrasound systems", in *Proc. of the IEEE Ultrasonics Symposium*, 2010, pp. 2286–2290.

[14] T. Darwich, C. Cavanaugh, "Amplitude Shifting for Sidelobes Cancellation Pulse Compression", in *Proc. of the International Conference on Radar*, 2006, pp. 1–4.

[15] M. Pollakowski, H. Ermert, "Chirp signal matching and signal power optimization in pulse-echo mode ultrasonic nondestructive testing", *IEEE Trans. on Ultrasonics, Ferroeletrics and Frequency Control*, vol. 41, no. 5, pp. 655–659, 1994. [Online]. Available: http://dx.doi.org/10.1109/58.308500

[16] R. J. Kazys, L. Svilainis, L. Mazeika, "Application of orthogonal ultrasonic signals and binaural processing for imaging of the environment", *Ultrasonics*, vol. 38, pp. 171–175, 2000. [Online]. Available: http://dx.doi.org/10.1016/S0041-624X(99)00078-5

[17] L. Svilainis, S. Kitov, A. Rodríguez, L. Vergara, et al., "Comparison of Spread Spectrum and Pulse Signal Excitation for Split Spectrum Techniques Composite Imaging", in *Proc. of the IOP Conference Series: Materials Science and Engineering*, 2012, to be published.

[18] L. Fortuna, M. Frasca, A. Rizzo, "Chaotic pulse position modulation to improve the efficiency of sonar sensors", *IEEE Trans. Instrum. and Meas.*, vol. 52, pp. 1809–1814, 2003. [Online]. Available: http://dx.doi.org/10.1109/TIM.2003.820452

[19] Z.-J. Yao, Q.-H. Meng, G.-W. Li, P. Lin, "Non-crosstalk real-time ultrasonic range system with optimized chaotic pulse position-width modulation excitation", in *Proc. of the IEEE Ultrasonics Symp.*, 2008, pp. 729–732.

[20] S. D. Blunt, T. Higgins, "Dimensionality Reduction Techniques for Efficient Adaptive Pulse Compression", *IEEE Trans. on Aerospace and Electronic Systems*, vol. 46, no. 1, pp. 349–362, 2010. [Online]. Available: http://dx.doi.org/10.1109/TAES.2010.5417167